arXiv:1108.4447v1 [quant-ph] 22 Aug 2011

Klein-Tunneling of a Quasirelativistic Bose-Einstein Condensate in an Optical Lattice

Tobias Salger,* Christopher Grossert,† Sebastian Kling, and Martin Weitz
Institut für Angewandte Physik der Universität Bonn, Wegelerstr. 8, 53115 Bonn

(Dated: August 24, 2011)

Optical lattices have proven to be powerful systems for quantum simulations of solid state physics effects. Here we report a proof-of-principle experiment simulating effects predicted by relativistic wave equations with ultracold atoms in a bichromatic optical lattice that allows for a tailoring of the dispersion relation. We observe the analog of Klein-tunneling, the penetration of relativistic particles through a potential barrier without the exponential damping that is characteristic for nonrelativistic quantum tunneling. Both linear (relativistic) and quadratic (nonrelativistic) dispersion relations are investigated, and significant barrier transmission is observed only for the relativistic case.

PACS numbers: 03.67.Ac, 03.65.Pm, 37.10.Jk, 67.85.Hj

Klein tunneling, a textbook effect in which relativistic particles penetrate through a potential barrier without the exponential damping that is characteristic for nonrelativistic quantum tunnelling [1, 2], has never been observed for elementary particles. In this counterintuitive consequence of relativistic quantum mechanics, a strong potential, being repulsive for particles and attractive for antiparticles, results in particle- and antiparticle-like states aligning in energy across the barrier. Therefore, a high transmission probability is expected when a potential drop of the order of the particles rest energy mc^2 is achieved over the Compton length h/mc. For electrons, one derives an extremely high required electric field strength of $\approx 10^{16}$V/cm, which so far has prevented an experimental realization on this system. The observation of Klein tunnelling has however been reported in solid state analogons [3–6], for example in graphene material. In this carbon material owing to a linear, i.e. quasirelativistic, dispersion relation around the Fermi edge, relativistic effects can be very illustratively emulated [3]. Other systems suitable for the simulation of quasirelativistic effects are ions with a long-lived two-component electronic structure in Paul traps [7], where the nonrelativistically forbidden entry into a high potential well has been observed [8]. Experiments in photonic structures [9] and in dark state media [10, 11] have been proposed. Ultracold atoms in optical lattices [12] allow for the investigation of both linear and nonlinear Hamiltonians due to the neutral charge of the atoms, with prospects including the simulation of interacting relativistic quantum field theories [13].

Here we report a proof-of-principle quantum simulation of relativistic wave equation predictions with ultracold atoms in an optical lattice. Our experiment is based on rubidium atoms in a Fourier-synthesized lattice potential consisting of an optical standing wave with spatial periodicity $\lambda/2$, where λ denotes the laser wavelength, and a higher spatial harmonic with $\lambda/4$ spatial periodicity. For a suitable choice of relative phases and amplitudes of the harmonics, the dispersion relation in the region between the first and second excited Bloch band becomes linear, as known for ultrarelativistic particles. We experimentally demonstrate both the transmission of atoms through a potential barrier for the case of a linear dispersion relation, i.e. Klein-tunneling, and the usual reflection of atoms by the barrier for the case of a quadratic, i.e. Schrödinger-like, dispersion in an excited Bloch band.

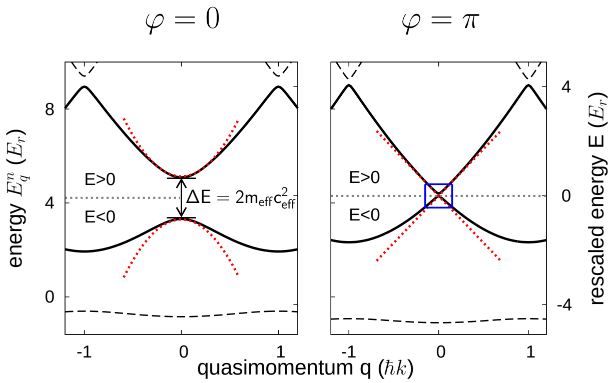

FIG. 1. Band structure for an optical lattice potential for a relative phase of $\varphi = 0$ (left) and $\varphi = \pi$ (right). The parameters for the lattice depths were $V_1 = 5E_r$ and $V_2 = 1.6E_r$. For $\varphi = \pi$ the splitting between the first and the second excited band vanishes, and a Dirac-point (marked by the solid blue box) is observed. The bands relevant for the experiment are shown by solid lines, and on the rescaled energy scale shown on the right hand side, zero energy is chosen at the position of the band crossing.

The periodic potential used to taylor the dispersion of ultracold rubidium atoms is of the form $V(z) = V_1/2\cos(2kz) + V_2/2\cos(4kz+\varphi)$, where $k = 2\pi/\lambda$ is the photon wavevector, V_1 denotes the potential depth of the usual standing wave potential and V_2 that of the higher spatial harmonic, generated by the dispersion of multiphoton Raman transitions [14, 15]. Fig. 1 shows the band structure for such a Fourier-synthesized lattice for $V_1 = 5E_r$ and $V_2 = 1.6E_r$ used in our experiment, where $E_r = \hbar^2k^2/2m$ denotes the recoil energy, for two different values of the relative phase φ between lattice harmonics. For the shown parameters, while the splitting between the first and the second excited Bloch band exhibits a nonzero value for $\varphi = 0$, it vanishes for a phase of $\varphi = \pi$. The critical dependence on the relative phase between lattice harmonics is understood in terms of the splitting arising from both contributions of second order Bragg scattering of the usual lattice and of first order Bragg scattering of the higher spatial harmonic, where the contributions interfere constructively or destructively depending on φ [15]. Of special interest is the case of destructive interference of the Bragg-scattering amplitudes, realized with $\varphi = \pi$ (see Fig. 1 right), for which at a suitable choice of lattice amplitudes the dispersion relation near the resulting crossing point becomes linear, i.e. relativistic, with an effective light speed $c_{\text{eff}} = 2\hbar k/m \simeq 1.1\text{cm/s}$ for the used 783nm laser wavelength. Both for vanishing and small splittings between the bands, we expect to be able to simulate relativistic physics, where a variation of the effective atomic Compton wavelength $\lambda_{\text{c,eff}} = h/m_{\text{eff}}c_{\text{eff}} = 2c_{\text{eff}}h/\Delta E$, with $m_{\text{eff}} = \Delta E/2c_{\text{eff}}^2$ as the effective mass and ΔE as the size of the splitting, is possible by appropriate choice of amplitude and phase values of the lattice harmonics. In the limit of $\Delta E \to 0$ the effective Compton wavelength diverges. If we choose the zero point of the energy scale to be at the crossing, atomic population in the second excited band (above the crossing) corresponds to a particle-like excitation, in the below lying band of negative energy according to the Stückelberg-Feynman interpretation to a particle-like excitation propagating backwards in time, which is equivalent to a temporally forward propagating antiparticle excitation [2]. Formally, the dynamics of atoms in the bichromatic lattice near the crossing between the first two excited bands can be described using a one-dimensional Dirac-like Hamiltonian (see [16] and Supplementary Material):

$$H = m_{\text{eff}}c_{\text{eff}}^2\sigma_z + c_{\text{eff}}\hat{q}\sigma_x + V_{\text{slow}}(z)\,, \tag{1}$$

where σ_x and σ_z are Pauli matrices, $\hat{q} = -i\hbar\delta_z$ is the momentum operator and $V_{\text{slow}}(z)$ is an external potential varying much slower than the lattice periodicity. The two-component Hamiltonian acts on spinors $\psi = (\psi_2, \psi_1)$, with ψ_1 and ψ_2 corresponding to course-grain atomic wave-functions in the upper and lower bands, respectively. Equation 1 becomes exact in the limit $|q| \ll \hbar k$ and $m_{\text{eff}}c_{\text{eff}}^2 \ll E_r$. One of the hallmark-effects of a relativistic dispersion is Klein-tunneling, which is a single-particle effect, so it can be equally well observed for bosons (as used in our experiment) and fermions [17].

In our experiment Klein-tunneling is investigated by monitoring the transmission through an external potential barrier that stands against the outcoupling of atoms from a far detuned optical dipole potential of depth V_0 by the earth's gravitational acceleration g. The spatial distribution of the combined potential $V_{\text{slow}}(z) = -V_0 \exp\left(-2\left(z/\omega_0\right)^2\right) - mgz$ is shown in Fig. 2c, where the height V_b of the potential barrier relatively to the minimum of the trapping potential can be adjusted by variation of the dipole trap beam power. The width of the potential barrier is of the same order as the used beam diameter $2\omega_0 \simeq 46\mu\text{m}$. For a typical atomic energy of one recoil energy below the maximum of the potential barrier, the estimated probability for usual nonrelativistic quantum tunneling is of the order $P_{\text{nr}} = \exp\left(-2\sqrt{2mE_r}z/\hbar\right) \simeq 10^{-170}$, i.e. completely negligible.

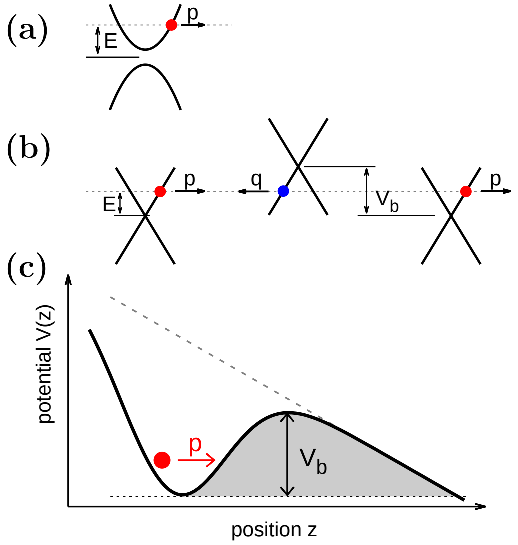

FIG. 2. Klein-tunneling of atoms through a potential barrier. (a) Relevant part of the dispersion relation in the lattice for a relative phase between lattice harmonics of $\varphi = 0$, for which the large splitting suppresses a tunneling between bands. (b) For $\varphi = \pi$ the dispersion relation is linear and the two Bloch bands touch each other. Shown in the three diagrams is the variation of the atomic energy during passage of a potential barrier of height V_b. (c) Spatial distribution of the combined potential formed by gravitational and dipole trapping potential. Atoms can pass the potential well in the case of $\varphi = \pi$ due to their possibility to drop to below the band crossing in the Bloch spectrum when loosing potential energy, see the middle graph in (b).

The situation however changes when quasirelativistic Klein-tunneling occurs, because the tunneling rate for this process does not decay exponentially with the width of the potential barrier. A quasirelativistic dispersion relation for ultracold rubidium atoms is induced using the Fourier-synthesized optical lattice, and Figs. 2a and 2b (left) indicate the relevant part of the atomic dispersion relation near the crossing between the first and the second excited Bloch-band for a relative phase of $\varphi = 0$ and $\varphi = \pi$. The atoms are loaded at a quasimomentum q well above the crossing region, but when proceeding towards the potential well on its rising edge loose kinetic energy, i.e. their momentum reduces. For a phase $\varphi = 0$, the splitting between the first and second excited Bloch-band is comparatively large (see Fig.2a). This results in a small effective Compton wavelength, $\lambda_{\mathrm{c,eff}} \approx 6\mu\mathrm{m}$, which is below the length of the rising edge of the barrier, and we expect no Landau-Zener tunneling into the lower band. The dispersion relation for atoms in the upper band then is Schrödinger-like. When the height of the potential barrier is larger than $q^2/2m_{\mathrm{eff}}$, the particle cannot pass through the barrier.

On the other hand, for a relative phase $\varphi = \pi$ between lattice harmonics, cf. Fig. 2b, the dispersion relation in the vicinity of the crossing point between the first and the second excited Bloch-band becomes ultrarelativistic. The effective Compton wavelength becomes larger than the widths of the edges of the barrier, and particles that approach the potential barrier and loose kinetic energy on the rising edge can be accelerated to below the crossing point between the second and the first excited Bloch-band (the Dirac-point), i.e. to states of negative energy of the energy scale shown in Fig.2c. Correspondingly, they can surpass higher potential barriers than in the nonrelativistic case of Fig. 2a. This corresponds to the case of Klein-tunneling. Our experiment simulates the conversion of a particle into a spatially backwards propagating antiparticle during the transmission of the barrier, whereafter the crossing point of bands again is passed on the tailing edge, so that particle-like states are again observed beyond the well. As in the case of the Klein-tunneling of electrons, this is equivalent to a double Landau-Zener passage between states of positive and negative energy respectively [2, 3].

The experiment proceeds by initially producing a Bose-Einstein condensate of rubidium atoms in an $m_F = 0$ spin projection of the $F = 1$ ground state within a dipole trapping potential formed by a focused $\mathrm{CO_2}$-laser beam. To prepare atoms in the second excited Bloch-band, we initially leave the atoms in ballistic free fall by extinguishing the $\mathrm{CO_2}$-laser dipole potential until the atoms have reached a momentum of $0.9\hbar k$ by the earths gravitational force, and then apply a Doppler-sensitive Raman pulse transferring atoms to the $m_F = -1$ spin projection and imparting two photon recoil momentum, which increases the momentum to its desired value of $2.9\hbar k$. This initial momentum allows to load atoms into the second excited Bloch-band of the lattice potential (at the position $q = 0.9\hbar k$), and the $\mathrm{CO_2}$-laser dipole potential required for the shaping of the desired slowly spatially varying potential barrier is again activated. The ballistic free fall during momentum preparation is about 2μm, i.e. well below the focal diameter of the trapping beam.

Fig.3a shows typical experimental data for the spatial atomic distribution, as recorded by absorption imaging at a time 5ms after preparation, for a relative phase $\varphi = 0$ and $\varphi = \pi$ between lattice harmonics respectively. The height of the potential barrier was $V_b = 5E_r$, while the average initial energy of the particle was $E = E_{\mathrm{kin}} + m_{\mathrm{eff}} c_{\mathrm{eff}}^2 = 3.9E_r$, with $m_{\mathrm{eff}} c_{\mathrm{eff}}^2$ of $0.5E_r$ and 0 for $\varphi = 0$ and $\varphi = \pi$, respectively (see also Fig. 1a).

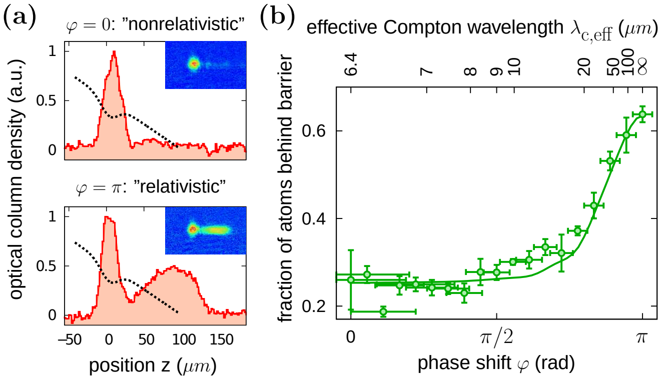

FIG. 3. (a) Cuts (solid red) through the measured spatial atomic distribution (insets) for a 5ms experiment time. Atoms proceeding from the center of the dipole trapping potential towards the potential barrier that detains against an outcoupling by the earths gravitational field for a relative phase between lattice harmonics of (top) $\varphi = 0$ and (bottom) $\varphi = \pi$. The dotted black line indicates the potential $V_{\mathrm{slow}}(z)$. (b) Relative atomic population beyond the potential barrier versus phase φ. The corresponding effective Compton wavelength $\lambda_{\mathrm{c,eff}} = 2c_{\mathrm{eff}}h/\Delta E$ is shown on the top scale. The shown horizontal error bars refer to the latter scale and are dominated by the uncertainty in ΔE, while the estimated uncertainty for the phase φ (lower scale) is below the drawing size of the dots. The solid line is the result of a numerical integration of the relativistic wave equation (see eq. (1)). The only free fit parameters were amplitude and offset.

The insets are false-colour shadow images of the atomic cloud, with the spot on the left-hand side corresponding to atoms near the trap location (i.e. before the barrier) and atoms on the right-hand side to particles that have transmitted the barrier. The solid red lines in the main images are cuts through the center, with the external potential indicated by dotted black lines. The data shows that for a relative phase of $\varphi = 0$, almost all atoms remain in front of the barrier, as expected. On the other hand, for $\varphi = \pi$, our experimental data show that most of the atomic population can be found beyond the potential barrier, equivalent to Klein-tunneling in this optical lattice system.

Note that for Klein-tunneling perfect transmission through the barrier is expected, when the energy splitting ΔE would be zero. In our experiment, some 30% of the population remains in front of the barrier, which we mainly attribute to atoms that did not take part in the Doppler-sensitive Raman transfer, and remain trapped in the $\mathrm{CO_2}$-laser beam focus. We have measured the atomic population found beyond the barrier for variable values of the phase φ between lattice harmonics, to investigate the case of intermediate values of the splitting ΔE between Bloch-bands. Corresponding data is displayed by the dots in Fig. 3b. The effective Compton wavelength becomes sufficiently large for Klein-tunneling only in a narrow region near $\varphi = \pi$, corresponding to the ultra-

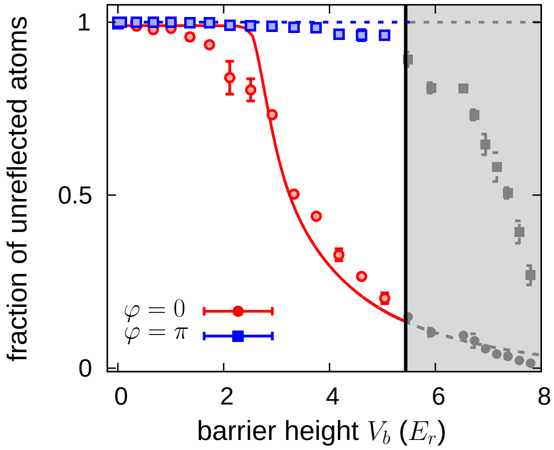

FIG. 4. Fraction of unreflected atoms versus the height of the potential barrier V_b for a phase shift (solid red) $\varphi = 0$ and (dashed blue) $\varphi = \pi$. The solid lines show numerical simulations. The grey shaded region corresponds to barrier height values where the atomic velocity reaches the edge of the Brillouin zone at $|q| = \hbar k$. The desired dispersion relation is reached only in the white region. The experimental parameters are the same as in Fig. 3a except for the barrier height.

relativistic case, while the atoms remain in front of the barrier for smaller phase values. The solid line is the result of a numerical simulation of the relativistic wave equation (see eq.1), in good agreement with the experimental data.

A striking prediction for Klein-tunneling is that the transmission through the barrier is expected to be independent of the barrier height, an issue in clear contrast to the expectations for nonrelativistic quantum mechanics. For a corresponding measurement in our system a momentum resolved time-of-flight measurement was employed to allow for a Stern-Gerlach separation of atoms that did not take part in the Raman transfer (see Supplementary Material). Fig.4 shows the relative signal of unreflected atoms, corresponding to Klein-tunneled atoms, versus the barrier height V_b. The grey shaded region corresponds to barrier height values where the atomic velocity reaches the edge of the lattice Brillouin zone at $|q| = \hbar k$, for which the bottom of the first exited band can be reached, i.e. only in the left white region the desired dispersion relation is achieved, with larger accuracy when remaining far from the shaded region. The blue squares are data recorded for $\varphi = \pi$, corresponding to a quasirelativistic dispersion, for which this signal remains at a high value within nearly the complete white region, illustrating the prediction of Klein-tunneling being independent of the barrier height with good accuracy. On the other hand, a pronounced loss of this signal at large barrier heights is observed for $\varphi = 0$ (red dots), corresponding to a nonrelativistic dispersion. Quantum tunnelling remains negligible due to the large spatial width of the barrier. The finite width of the kinetic atomic energy distribution here softens the otherwise expected sharp decay for $E_{\text{kin}} < V_b$. The shown solid and dashed lines are the result of a numerical simulation, which for the relativistic case are in good agreement with the data and also qualitatively reproduce the nonrelativistic case.

To conclude, we report an experiment demonstrating the analog of Klein-tunneling, as a proof-of-principle experiment testing relativistic wave equation predictions, with ultracold atoms in a bichromatic optical lattice. By tuning the relative phase between lattice harmonics the atomic dispersion can be tuned continuously from the nonrelativistic to the ultrarelativistic case, though the atoms move at a velocity 10 orders of magnitude below the speed of light.

For the future, we expect that ultracold atoms in optical lattices allow quantum simulations of a wide range of effects of both linear and nonlinear Dirac-dynamics. Perspectives include the verification of theoretical high energy physics predictions [18], as chiral confinement, and other results of massive Thirring models [13, 19, 20].

Financial support of the DFG is acknowledged. We thank A. Rosch, L. Santos, D. Witthaut, H. Kroha, and K. Ziegler for discussions.

---

[*] salger@iap.uni-bonn.de
[†] grossert@iap.uni-bonn.de

[1] 0.Klein, Z.Phys **53**, 157 (1929).
[2] See, e.g.: J. Bjorken, S. Drell, *Relativistic Quantum Mechanics* (Mc Graw-Hill, New York, 1964).
[3] M.I. Katsnelson, K.S. Novoselov, A.K. Geim, Nature Phys. **2**, 620 (2006).
[4] A.F. Young, P. Kim, Nature Phys. **5**, 222 (2009).
[5] N. Stander, B. Huard, D. Goldhaber-Gordon, Phys. Rev. Lett **102**, 026807 (2009).
[6] G.A. Steele, G. Gotz, L.P. Kouwenhoven, Nature Nanotechnology **4**, 363 (2009).
[7] R. Gerritsma et al., Nature **463**, 68 (2010).
[8] R. Gerritsma et al., Phys. Rev. Lett **106**, 060503 (2011).
[9] S. Longhi, Phys. Rev. B **81**, 075102 (2010).
[10] G. Juzeliunas et al. Phys. Rev. A **77**, 011802 (2008).
[11] J.Y. Vaishnav, C.W. Clark, Phys. Rev. Lett **100**, 153002 (2008).
[12] I. Bloch, J. Dalibard, W. Zwerger, Rev. Mod. Phys. **80**, 885 (2008).
[13] J.I. Cirac, P. Maraner, J.K. Pachos, Phys. Rev. Lett. **105**, 190403 (2010).
[14] G. Ritt et al., Phys. Rev. A **74**, 063622 (2006).
[15] T. Salger, C. Geckeler, S. Kling, and M. Weitz, Phys. Rev. Lett. **99**, 190405 (2007).
[16] D. Witthaut et al., Phys. Rev. A (in press).
[17] H. Feshbach, F. Villars, Rev. Mod. Phys. **30**, 24 (1958).
[18] M. Merkl et al., Phys. Rev. Lett. **104**, 073603 (2010).
[19] S.-J. Chang, S.D. Ellis, B.W. Lee, Phys. Rev. D **11**, 3572 (1975).
[20] S.Y. Lee, T.K. Kuo, A. Gavrielides, Phys. Rev. D **12**, 2249 (1975).